EVALUATING INDUCTIVE PARAMETER-BASED TRANSFER LEARNING WITH DEEP NEURAL NETWORKS FOR WIND FORECASTING IN CORSICA

Anonymous authors

Paper under double-blind review

ABSTRACT

This study assesses the effectiveness of various transfer learning strategies for wind speed forecasting across meteorological stations in Corsica using deep neural networks. Leveraging inductive parameter-based transfer, models are transferred based on geographic proximity, topographic classification, dominant wind direction, and random assignment. Several architectures are evaluated, including recurrent, convolutional, attention-based, and dense networks. Results indicate that structured transfer strategies do not consistently outperform non-transfer baselines. This lack of improvement can be largely attributed to significant distributional differences in wind speed across stations, which hinder model transferability. These findings highlight the challenges posed by domain shift in a geographically heterogeneous insular context and emphasize the need for more refined similarity criteria, hybrid transfer strategies, and spatially-aware modeling, notably through graph neural networks. The results also call for a critical reassessment of commonly held assumptions about the benefits of transfer learning in complex meteorological environments.

1 Introduction

Accurate wind speed forecasting is a critical challenge for various industrial and environmental applications, particularly in the management of renewable energy and the mitigation of climate-related risks Jiang et al. (2021); Khodayar et al. (2017). However, the comprehensive collection of high-resolution meteorological data remains complex, especially in regions such as Corsica. Transfer learning, by reusing models previously trained on similar source domains, offers a promising approach to overcome these constraints while reducing computational costs Wellens et al. (2021). It provides a methodological response to the limitations of conventional supervised learning, particularly in contexts with limited labeled data, feature space divergences, or distribution mismatches between training and testing sets Gholizade et al. (2025). By leveraging a model pre-trained on a source domain, transfer learning enables improved performance on a target domain while reducing data requirements and computational costs Sankari & Kumar (2023).

Several taxonomies have been proposed to structure the literature on transfer learning. From the perspective of the *label space*, three paradigms are typically distinguished: *inductive* transfer, involving labeled data in both domains; *transductive* transfer, where only the source data are labeled; and *unsupervised* transfer, where no labels are available Gholizade et al. (2025). The relationship between these paradigms and the similarity between source and target domains has been emphasized in previous studies Sankari & Kumar (2023). In terms of the feature space, a distinction is made between *homogeneous* settings, where the features are identical but may differ in distribution, and *heterogeneous* settings, where the feature spaces differ Gholizade et al. (2025); Sankari & Kumar (2023).

Transfer mechanisms can also be categorized by the nature of the transferred knowledge. The main approaches include: (i) *instance-based transfer*, which involves selecting or reweighting relevant source examples; (ii) *feature-based transfer*, aiming to project data into a common representative space; (iii) *parameter-based transfer*, which reuses weights from a source model; and (iv) *relation-based transfer*, which exploits structural similarities between domains Gholizade et al. (2025); Al-

Hajj et al. (2023). In all cases, the chosen strategy depends on data availability, task similarity, and the application domain. A poor alignment between source and target can lead to *negative transfer*, resulting in degraded performance Zhang et al. (2021).

In the field of wind speed forecasting, transfer learning has been used to address dataset heterogeneity across sites or tasks. For instance, Qureshi & Khan (2018) introduced an inter-site framework based on sparse autoencoders guided by a deep belief network. This adaptive system (ATL-DNN) dynamically adjusts the transferred representations according to local characteristics. Oh et al. (2022) proposed an approach involving partial layer sharing in a C-LSTM model, demonstrating accuracy improvements for data-scarce sites. In an instance-based transfer context, Cai et al. (2019) proposed a source selection mechanism to mitigate negative transfer effects and improve quantile forecasting via GBDT. Task transfer has also been explored: Qureshi & Khan (2018) studied the transition from power to wind speed prediction, while Chen (2022) employed *knowledge distillation* to transfer representations from a complex teacher model to a lightweight student model.

Regarding *neural architectures*, several families have been adopted in these approaches. Recurrent networks such as LSTM and BiLSTM are employed for their ability to model temporal dependencies Oh et al. (2022); Chen (2022), while autoencoders are used to produce compressed and transferable latent representations Qureshi & Khan (2018); Oh et al. (2022). Additionally, some contributions combine transfer learning with ensemble models such as GBDT Cai et al. (2019) or optimized Adaboost Chen (2022), highlighting the complementarity between statistical robustness and generalization capacity.

Overall, these works converge on a common goal: maximizing predictive performance in low-data scenarios while reducing the computational resources required for model training. It is within this perspective that our contribution is situated, leveraging transfer learning to reduce the size of training datasets needed in meteorological contexts, and thereby decreasing the computational costs associated with predictive model training.

This study presents an analysis of structured transfer learning strategies applied to wind speed prediction across a network of meteorological stations in Corsica. We specifically compare strategies based on distance, topographic classification, directional wind speed dominance, and random transfer against the same neural architecture without transfer learning. Several neural architectures are evaluated, encompassing multiple paradigms: recurrent networks, convolutional-recurrent networks, multi-layer perceptrons (dense), and attention mechanisms.

2 Data

This section presents the dataset used in our study, comprising time series of wind speed measurements collected from multiple meteorological stations, as well as the preprocessing procedures applied to ensure the quality and consistency of the data before their integration into the predictive models. All station data originate from official Météo France records available at : meteo.data.gouv.fr

2.1 STATION DISTRIBUTION

Our study is based on the analysis of meteorological stations located throughout the island of Corsica. These stations are represented as red dots in Figure 1 left part.

Out of the 98 existing stations, we selected 22 based on two main criteria: the availability of wind speed measurements and the length of their historical time series. Specifically, we retained stations with more than 80,000 hours of data (approximately 9 years), ensuring significant temporal continuity and minimizing the need for interpolation. This threshold was determined through a comparative analysis of all available stations: a distinct group stood out with dense and regular temporal coverage, whereas others exhibited frequent and substantial gaps in their records.

The right part of figure 1 illustrates Corsica's topography using a color-coded altitude map. This visualization highlights the island's geographical diversity, notably the alternation between coastal areas and mountainous regions, which are major factors influencing wind dynamics Grante et al. (2025). The location of the meteorological stations was analyzed in relation to this topography to ensure good representativeness across different geographical contexts.

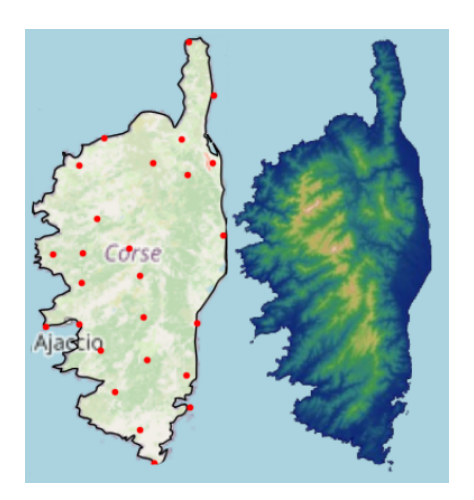


Figure 1: Weather Stations Distribution and Topography of Corsica

2.2 FEATURES

The meteorological variables used in our study are listed in Table 1. These constitute the main input features for our predictive models and were selected in line with prior work such as Ryu et al. (2022); Yang et al. (2023); Tang et al. (2020); Geng et al. (2020).

Table 1: Features of the meteorological station dataset

Name	Units	Description		
FF	$m.s^{-1}$	Wind speed		
DD_{cos}	none	Cosine of wind direction (FF)		
DD_{sin}	none	Sine of wind direction (FF)		
FXI	$m.s^{-1}$	Maximum wind speed		
U	%	Relative humidity		
T	$^{\circ}C$	Temperature at 2 meters		

We additionally included four features to decompose the day and hour of measurement, enabling non-temporally-optimized models to better capture temporal dynamics Baile & Muzy (2022). Furthermore, two features were added to better represent wind direction. Since the wind direction angle *DD* ranges from 0 to 360°, values like 1° and 359° are close in physical meaning but numerically distant. We chose to encode this circular characteristic directly in the input features.

For S, the vector representing temporal features, we define:

$$S = [S_1, S_2, S_3, S_4] = \left[\cos\left(2\pi \frac{h}{24}\right), \sin\left(2\pi \frac{h}{24}\right), \cos\left(2\pi \frac{d}{365.25}\right), \sin\left(2\pi \frac{d}{365.25}\right)\right] \tag{1}$$

where h is the hour of the day and d is the day of the year.

For the wind direction DD, we compute:

$$\theta = \pi \frac{\text{DD}}{180} \tag{2}$$

then

$$DD_{\cos} = \cos(\theta), \quad DD_{\sin} = \sin(\theta)$$
 (3)

The final input dataset is composed as follows:

$$X = [FF, DD_{cos}, DD_{sin}, FXI, U, T, S_1, S_2, S_3, S_4]$$
 (4)

Each station has its own dataset, denoted $X_{station}$. For each $X_{station}$, missing values were linearly interpolated. Subsequently, we standardized FF, FXI, U, and T to align their scales and to improve

training efficiency and stability by reducing overfitting. Variables from the vector S as well as DD_{\sin} and DD_{\cos} are already bounded in the range [-1,1] and thus were not normalized or standardized.

3 METHODOLOGY

This section presents the deep learning models used for wind speed forecasting, as well as the various transfer learning strategies employed.

3.1 METRICS

The root mean square error (RMSE) was selected as the evaluation metric for this study. It is generally defined as:

RMSE =
$$\sqrt{\frac{1}{n} \sum_{i=1}^{n} (y_i - \hat{y}_i)^2}$$
 (5)

It represents the average Euclidean distance between the true value y and the model prediction \hat{y} . This metric penalizes larger errors more heavily, making it sensitive to outliers. A low RMSE indicates that the model predictions are close to the true values, while a high RMSE reflects significant discrepancies between predictions and observations.

In order to evaluate the effectiveness of the transfer learning strategies, we compare them to an identical architecture trained without transfer over the same historical period. The gain is defined as the relative reduction in the RMSE, expressed as a percentage:

$$Gain (\%) = \frac{RMSE_{reference} - RMSE_{transfer}}{RMSE_{reference}} \times 100$$
 (6)

3.2 Models

This subsection introduces the neural architectures selected for comparative analysis. Figure 2 provides a visual representation of the models implemented in this study. Our selection spans a broad range of neural network paradigms, including a Convolutional-LSTM model combining convolutional and recurrent networks, a Convolutional-Dense model integrating convolutional layers with fully connected layers, encoder architectures using the attention mechanism from the Transformer encoder Vaswani et al. (2017), standard LSTM architectures representing recurrent networks Hochreiter & Schmidhuber (1997), and feed-forward neural networks (FFN).

In our approach, all convolutional neural network architectures process the meteorological time series through one-dimensional (1D) convolutions, a choice dictated by the inherently sequential nature of the data. This technical decision aligns with the temporal structure of the variables, where local correlations manifest along the time axis. To ensure a fair comparison while preserving the structural integrity of each model, architectural characteristics (network depth, neuron density, dimensionality of hidden layers) were individually calibrated. This differentiated approach avoids enforcing parametric uniformity across models.

3.3 Transfer Learning

For this comparative study, we focused on inductive transfer learning strategies using parameter transfer by reusing and adjusting the weights of models previously trained (fine-tuning). Since each station has its own forecasting model, we transferred knowledge from one station to another. We compared four geographically informed transfer strategies:

- 1. Random transfer
- 2. Topographic classification-based transfer
- 3. Distance-based transfer
- 4. Dominant wind direction-based transfer

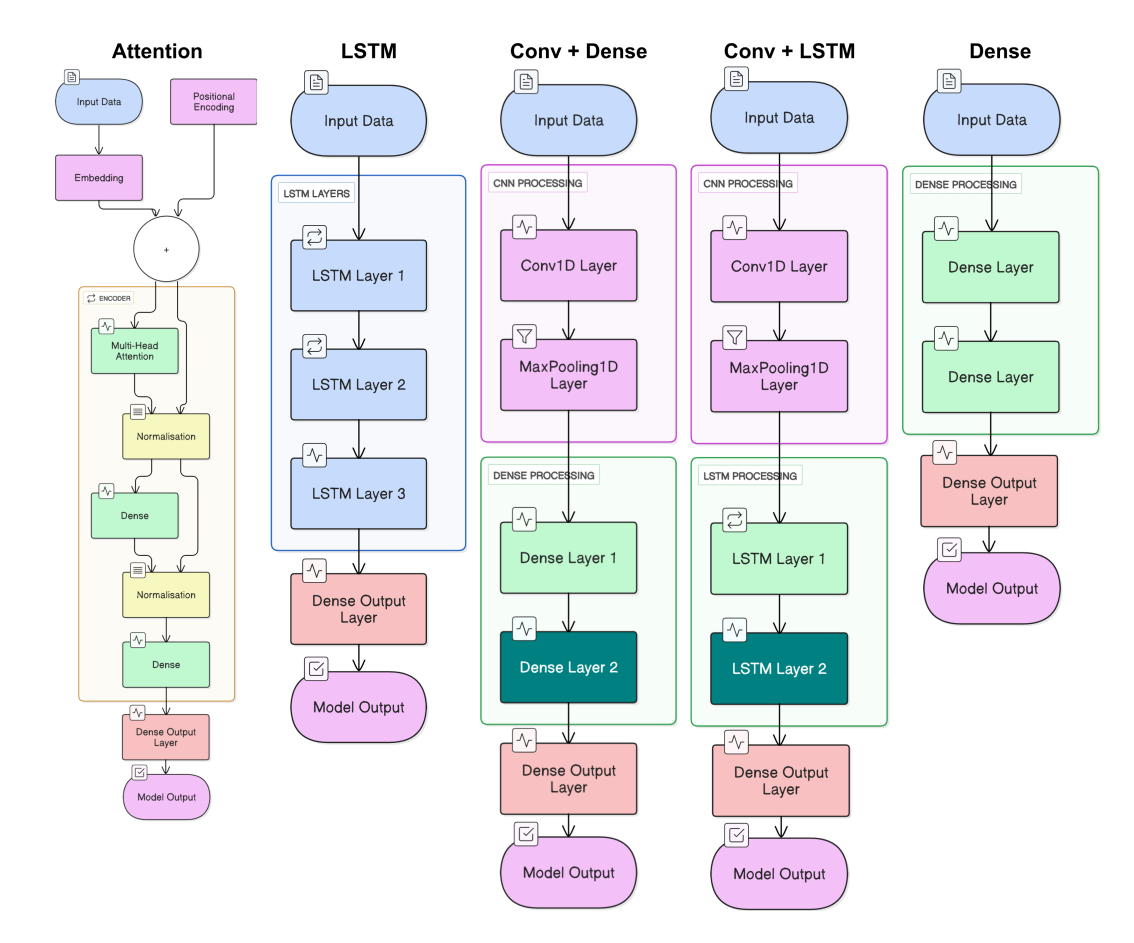


Figure 2: Architecture of the models used

Random transfer is used as a second baseline for evaluating the effectiveness of the transfer strategies. If a transfer strategy fails to outperform random transfer in terms of RMSE, its relevance and ability to leverage structural similarities between stations is questionable. Conversely, a significantly lower RMSE compared to random transfer supports the quality of the considered strategy.

For the topographic classification-based transfer, we initially distinguished three terrain types: mountain, plain, and coastal. However, a joint analysis of the map and the island's topography led us to merge the plain and coastal categories due to their strong topographic correlation. This resulted in a binary classification between mountain and plain-coast zones, using an altitude threshold of 300 meters. The central panel of Figure 3 illustrates this classification, where stations below the threshold are shown in blue (plain-coast), and those above in red (mountain).

For the distance-based transfer, knowledge is transferred to minimize the distance between source and target stations, as shown on the left panel of Figure 3. For each target station, we select the three nearest source stations using the Haversine distance between two geographical points (ϕ_1, λ_1) and (ϕ_2, λ_2) , defined as:

$$d = 2R \cdot \arcsin\left(\sqrt{\sin^2\left(\frac{\phi_2 - \phi_1}{2}\right) + \cos(\phi_1) \cdot \cos(\phi_2) \cdot \sin^2\left(\frac{\lambda_2 - \lambda_1}{2}\right)}\right)$$
(7)

where:

- ϕ_1, ϕ_2 are the latitudes in radians,
- λ_1, λ_2 are the longitudes in radians,
- R is the Earth's radius,

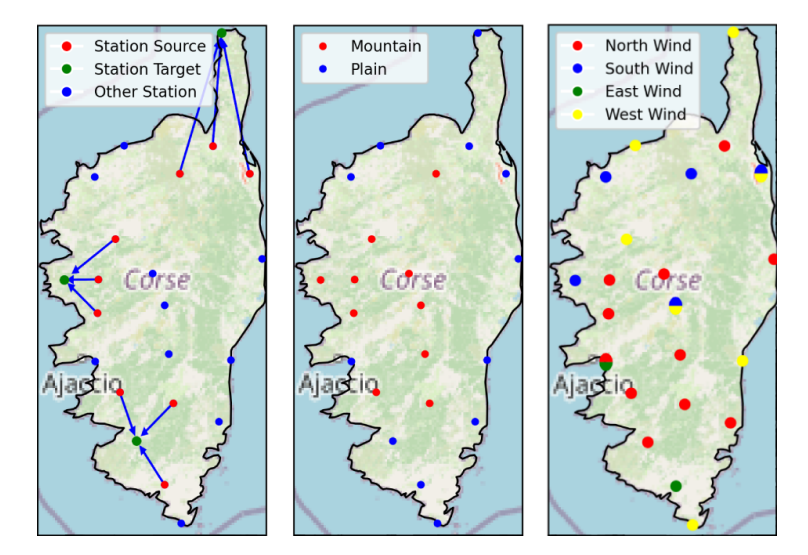


Figure 3: Map of meteorological stations. Left: visualization of transfers between stations. Target stations are shown in green, source stations in red, and other stations in blue. Blue arrows represent transfers from source to target stations. Center: topographic classification of stations. Mountain stations are shown in red; plain/coastal stations in blue. Right: station classification according to dominant wind directions in the study area. Stations are color-coded according to their dominant wind direction: red for north, blue for south, green for east, and yellow for west. Bi-colored stations correspond to cases where the prevailing wind lies between two cardinal directions (e.g., northeast), and are therefore classified into both associated directions.

• d is the distance between the two points.

For the dominant wind direction-based classification, stations were grouped according to the most frequent wind direction over the full observation period. When a station exhibited two dominant directions of comparable intensity, it was assigned to both groups. The right panel of figure 3 illustrates the spatial distribution of stations according to this classification. Bicolored points represent stations associated with two dominant directions. A station with a wind rose showing a shared maximum between north and northeast is considered as exposed to a northerly wind only. The same applies to other intercardinal directions.

Let E denote the set of all stations. Each strategy defines a subset $E' \subseteq E$ on which the transfer is applied. The transfer occurs in a random order among stations in E': a source station A can transfer its knowledge to a target station B if and only if $A, B \in E'$. The source model is a neural network with the same architecture, trained on the full training dataset of station A.

3.4 EXPERIMENTATION

The models are trained using the Adam optimizer with an initial learning rate of 10^{-3} . During fine-tuning — the adaptation phase of a model pre-trained on another station — the learning rate is reduced to 10^{-4} to promote more stable convergence. In practice, fine-tuning was conducted year by year, progressively extending the historical window: starting from 2020–2020, then 2019–2020, 2018–2020, and so forth, up to 2015–2020. For clarity, we report only the two extreme cases (2020–2020 and 2015–2020). When computing the gain of transfer learning defined in equation 6 with respect to the reference model, the baseline is always trained on the same historical window as the fine-tuned model. Training runs for up to 50 epochs, with early stopping based on validation loss and a patience of 5 epochs.

Performance is evaluated on an independent test set covering the period from 01/01/2023 to 31/12/2023. The validation set spans the year 2022. The training set varies depending on the target year and may extend from 01/01/2015 to 31/12/2021, for a maximum of seven years. Models operate with a sliding input window based on a history of three time steps.

Table 2: Summary of average performance per architecture / strategy pair from (h+1 to h+24): mean of RMSE and gain in % with fine-tuning performed using either 2015 (data from 2015–2020) or 2020 (data from 2020–2020) as historical year.

M - 1-1	Cturtores	DMCE 2015	DMCE 2020	C-:- 2015 (01)	C-:- 2020 (#)
Model	Strategy	RMSE 2015	RMSE 2020	Gain 2015 (%)	Gain 2020 (%)
attention	distance	0.8423	0.8561	-0.33	-0.63
attention	east	0.8702	0.8835	-3.65	-3.85
attention	mountain	0.8353	0.8532	0.50	-0.30
attention	north	0.8207	0.8343	2.25	1.92
attention	west	0.8447	0.8566	-0.62	-0.69
attention	plain	0.8371	0.8516	0.29	-0.11
attention	random	0.8373	0.8558	0.27	-0.60
attention	south	0.8604	0.8688	-2.49	-2.13
conv_dense	distance	0.8448	0.8579	-0.47	-0.47
conv_dense	east	0.8731	0.8859	-3.83	-3.74
conv_dense	mountain	0.8427	0.8559	-0.22	-0.23
conv_dense	north	0.8243	0.8417	1.96	1.42
conv_dense	west	0.8482	0.8608	-0.87	-0.81
conv_dense	plain	0.8414	0.8563	-0.07	-0.28
conv_dense	random	0.8404	0.8575	0.05	-0.42
conv_dense	south	0.8642	0.8740	-2.78	-2.36
dense	distance	0.8489	0.8654	-1.03	-1.61
dense	east	0.8688	0.8804	-3.39	-3.38
dense	mountain	0.8396	0.8552	0.08	-0.42
dense	north	0.8239	0.8441	1.95	0.89
dense	west	0.8480	0.8569	-0.91	-0.62
dense	plain	0.8393	0.8587	0.12	-0.84
dense	random	0.8404	0.8637	-0.01	-1.42
dense	south	0.8609	0.8753	-2.45	-2.78
conv_lstm	distance	0.8466	0.8620	-0.90	-0.99
conv_lstm	east	0.8737	0.8864	-4.12	-3.86
conv_lstm	mountain	0.8405	0.8550	-0.17	-0.17
conv_lstm	north	0.8232	0.8403	1.90	1.55
conv_lstm	west	0.8474	0.8596	-0.99	-0.72
conv_lstm	plain	0.8417	0.8558	-0.31	-0.27
conv_lstm	random	0.8404	0.8610	-0.16	-0.87
conv_lstm	south	0.8635	0.8705	-2.91	-2.00
lstm	distance	0.8474	0.8625	-1.05	-1.24
lstm	east	0.8693	0.8852	-3.66	-3.89
lstm	mountain	0.8410	0.8601	-0.28	-0.95
lstm	north	0.8226	0.8446	1.92	0.86
lstm	west	0.8463	0.8628	-0.91	-1.27
lstm	plain	0.8394	0.8553	-0.09	-0.39
lstm	random	0.8385	0.8627	0.02	-1.26
lstm	south	0.8616	0.8742	-2.74	-2.60

The models are designed to perform multi-step forecasting of wind speed (FF) over a 24-hour horizon. Specifically, each model produces a sequence of 24 predictions corresponding to hourly lead times from h+1 to h+24. This direct forecasting strategy enables the models to generate the entire prediction horizon in a single forward pass. Performance metrics are computed globally over the 24 forecast steps.

4 RESULTS

Table 2 summarizes the performance obtained for each architecture–strategy pair. For each combination, the table reports the mean RMSE and the mean gain defined in equation 6 with respect to the non-transfer baseline, averaged over horizons from h+1 to h+24 and computed under two historical windows (2015–2020 vs 2020 only).

Several clear tendencies emerge. First, the majority of strategies lead to either negligible or negative gains, with some configurations showing systematic performance degradation. This effect is particularly visible for directional dominant wind speed groupings such as East and South, which consistently result in average losses exceeding -2.00% across all architectures. Random selection, distance-based grouping and west also perform poorly, with mean relative gains close to zero or negative, reflecting unstable behavior.

In contrast, the North strategy stands out as the only configuration that provides positive average gains across all tested architectures. While these improvements remain modest (generally between +0.86% and +2.25%). This suggests that under specific transfer conditions, it is possible to mitigate

the negative effects observed elsewhere. Strategies based on topographic classification (mountain and plain) show intermediate results: they do not yield clear benefits, but their performance degradation remains less severe than for other directional groupings.

Overall, the table highlights the absence of a universally effective transfer strategy. Gains remain limited in magnitude and often offset by frequent negative transfers. Increasing the dataset size leads to better performance, although the improvements remain negligible in most cases. These findings confirm that, in the present setting, transfer learning cannot be considered a reliable approach for systematically improving model performance.

5 DISCUSSION

Our study investigates several transfer learning strategies aimed at improving wind speed prediction performance between different meteorological stations in Corsica. In contrast to a substantial body of literature reporting significant improvements through transfer learning Oh et al. (2022); Zhu et al. (2025); Zhang et al. (2024), our results show that structured transfer based on topographic or wind-directional criteria does not systematically offer a significant advantage over the non-transfer baseline strategy.

More fundamentally, our findings suggest that the tested transfer strategies do not significantly outperform models trained without any transfer, using only station-specific data. This observation calls into question the actual utility of transfer learning in the specific context of our study. While numerous previous works emphasize the effectiveness of transfer learning for boosting predictive performance, our results do not support such conclusions.

A key explanation for this discrepancy lies in the complex topography of Corsica and its strong influence on wind regimes. Meteorological stations are embedded in highly heterogeneous environments, which translates into markedly different data distributions. To better characterize these differences, we analyzed inter-station distributional distances of wind speed across the entire network. This divergence is clearly illustrated by the heatmap in figure 4, which highlights strong station-to-station variability. A Kolmogorov–Smirnov test was applied to all station pairs and further confirms substantial distributional wind speed shifts between groups of stations. According to Zhang et al. (2021), transfer learning is only expected to be effective when source and target domains share sufficiently similar distributions. In our case, this fundamental assumption is not respected, which can explains the recurrent negative transfer observed.

This result raises a broader methodological concern. Much of the existing literature on transfer learning reports striking performance gains, but often in contexts where distributional mismatches are less pronounced or not assessed. Our findings show that even a distributional shift—let alone the substantial ones induced by mountainous terrain—can undermine transfer effectiveness. In practice, this means that in highly variable regions such as Corsica, where local topographic effects dominate wind patterns, transfer learning may simply fail to deliver improvements. Transferred models may get stuck in local minima due to the mismatch between source and target distributions, limiting their ability to adapt effectively to the target station's specific characteristics.

Beyond this observation, the aggregation of stations into broad categories (e.g., "plain" and "coastal") may have further diluted local characteristics, masking more nuanced interactions and exacerbating negative transfer effects. A finer-grained, station-specific analysis would be necessary to determine whether any transfer configurations can yield consistent benefits. While forecasting up to h=24 provides a comprehensive view of daily wind speed evolution, predictive accuracy generally tends to degrade with increasing lead times, which may limit the reliability of long-horizon forecasts in operational settings.

Future work could incorporate temporal cross-validation and multi-year testing to enhance the generalization and robustness of predictions up to h+6. This recommendation echoes concerns about the existence of a performance floor for predictive models applied to meteorological data, due in part to the inherent complexity of local wind dynamics Baile & Muzy (2022). Another promising direction would be to explore hybrid transfer methods, such as the combined use of instance-based and parameter-based transfer, to better tailor transfer relevance to each specific context. Finally, extending models to explicitly integrate spatial information—such as through the use of graph neural networks—may further improve performance by leveraging spatial correlations between stations

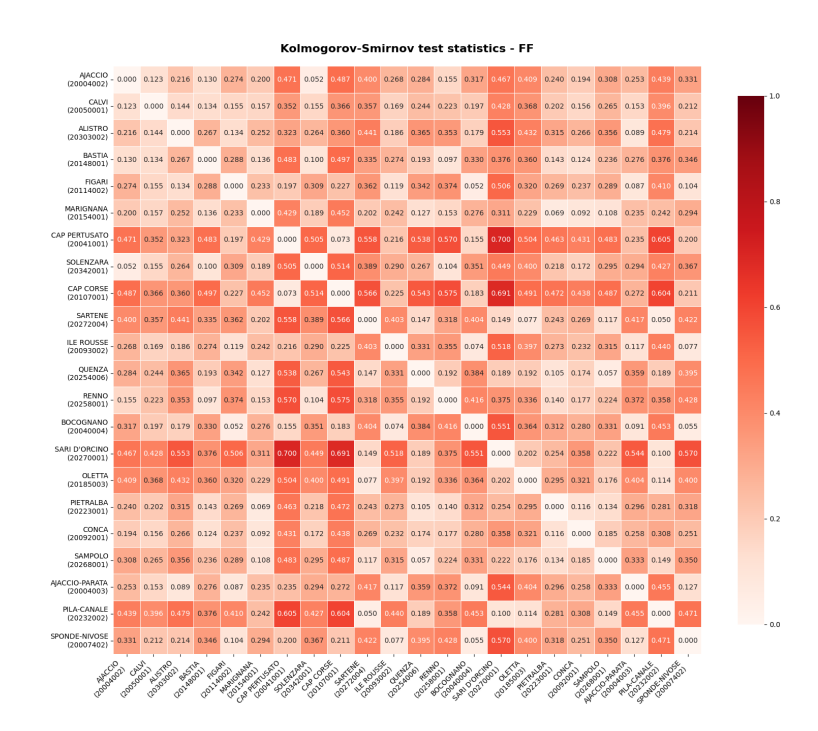


Figure 4: Heatmap of Kolmogorov–Smirnov test statistics highlighting inter-station distributional shifts in wind speed.

Khodayar & Wang (2019). In addition, meta-learning represents a promising avenue for enabling models to rapidly adapt to new stations with limited historical data, and will be explored in future work as a potential extension of the current transfer learning framework.

6 Conclusion

This study evaluated multiple transfer learning strategies for wind speed forecasting in Corsica. Contrary to much of the literature, our results show that transfer learning does not systematically improve performance and often induces negative transfer. The main reason lies in the strong distributional wind speed heterogeneity between stations, driven by complex topography, as confirmed by KS tests. This not respect the assumption of source–target similarity Zhang et al. (2021), explaining the recurrent failures of transfer.

These findings call for caution: transfer learning cannot be assumed universally beneficial, especially in geographically heterogeneous contexts. Additionally, transferred models may converge toward suboptimal solutions that do not align well with the specific dynamics of the target station. Future work should prioritize distribution-aware strategies, hybrid approaches, h+6 forecasting, and spatially explicit models such as graph neural networks, while also reporting negative results to avoid overly optimistic conclusions. Meta-learning techniques should also be explored to improve model adaptability.

REFERENCES

Rami Al-Hajj, Ali Assi, Bilel Neji, Raymond Ghandour, and Zaher Al Barakeh. Transfer learning for renewable energy systems: A survey. *Sustainability*, 15(11):9131, 2023.

Rachel Baile and J. F. Muzy. Leveraging data from nearby stations to improve short-term wind speed forecasts. *Elsevier*, 2022.

- Long Cai, Jie Gu, Jinghuan Ma, and Zhijian Jin. Probabilistic wind power forecasting approach via instance-based transfer learning embedded gradient boosting decision trees. *Energies*, 12(1):159, 2019.
 - Hao Chen. Knowledge distillation with error-correcting transfer learning for wind power prediction. *arXiv preprint arXiv:2204.00649*, 2022.
 - D. Geng, H. Zhang, and H. Wu. Short-term wind speed prediction based on principal component analysis and lstm. *Applied Sciences*, 10(13):4416, 2020.
 - Masoume Gholizade, Hadi Soltanizadeh, Mohammad Rahmanimanesh, and Shib Sankar Sana. A review of recent advances and strategies in transfer learning. *International Journal of System Assurance Engineering and Management*, pp. 1–40, 2025.
 - Diego Grante, Rachel Baile, and Christophe Paoli. Exploiter le deep learning pour prévoir les vitesses de vent: Une approche liant topographie et données de réanalyse météorologique. In *Extraction et Gestion des Connaissances (EGC'2025)*, 2025.
 - Sepp Hochreiter and Jürgen Schmidhuber. Long short-term memory. *Neural Computation*, 9(8): 1735–1780, 1997.
 - Ping Jiang, Zhenkun Liu, Xinsong Niu, and Lifang Zhang. A combined forecasting system based on statistical method, artificial neural networks, and deep learning methods for short-term wind speed forecasting. *Energy*, 223:119361, 2021. doi: 10.1016/j.energy.2020.119361.
 - Mahdi Khodayar and Jianhui Wang. Spatio-temporal graph deep neural network for short-term wind speed forecasting. *IEEE Transactions on Sustainable Energy*, 10:670–681, 2019.
 - Mehdi Khodayar, Mohammad Reza Bidram, Mohammad Ebrahim Hamedani Golshan, and Mohsen Khodayar. Rough deep neural architecture for short-term wind speed forecasting. *IEEE Transactions on Industrial Electronics*, 64(10):7650–7657, 2017. doi: 10.1109/TIE.2017.2682039.
 - JeongRim Oh, JongJin Park, ChangSoo Ok, ChungHun Ha, and Hong-Bae Jun. A study on the wind power forecasting model using transfer learning approach. *Electronics*, 11(24):4125, 2022.
 - Aqsa Saeed Qureshi and Asifullah Khan. Adaptive transfer learning in deep neural networks: Wind power prediction using knowledge transfer from region to region and between different task domains. *arXiv e-prints*, pp. arXiv:1810, 2018.
 - Ju-Yeol Ryu, Bora Lee, Sungho Park, Seonghyeon Hwang, Hyemin Park, Changhyeong Lee, and Dohyeon Kwon. Evaluation of weather information for short-term wind power forecasting with various types of models. *Energies*, 15(24):9403, 2022.
 - S. Siva Sankari and P. Senthil Kumar. A review of deep transfer learning strategy for energy forecasting. *Nature Environment and Pollution Technology*, 22(4):1781–1793, 2023.
 - Bin Tang, Yan Chen, Qin Chen, and Mengxing Su. Research on short-term wind power forecasting by data mining on historical wind resource. *Applied Sciences*, 10(4):1295, 2020.
 - Ashish Vaswani, Noam Shazeer, Niki Parmar, Jakob Uszkoreit, Llion Jones, Aidan N. Gomez, Łukasz Kaiser, and Illia Polosukhin. Attention is all you need. In *Advances in Neural Information Processing Systems (NeurIPS)*, volume 30, 2017.
 - Arnoud P. Wellens, Maxi Udenio, and Robert N. Boute. Transfer learning for hierarchical forecasting: Reducing computational efforts of m5 winning methods. *International Journal of Forecasting*, 2021. To appear.
 - Mao Yang, Yunfeng Guo, and Yutong Huang. Wind power ultra-short-term prediction method based on nwp wind speed correction and double clustering division of transitional weather process. *Energy*, 282:128947, 2023.
 - Jun Zhang, Yaoran Chen, Hang Pan, Liyuan Cao, and Chunxiang Li. Constrained deep reinforcement transfer learning for short-term forecasting of wind discrepancies at ocean stations. *SSRN Electronic Journal*, 2024. URL https://ssrn.com/abstract=5033497. Preprint.

W. Zhang, L. Deng, L. Zhang, and D. Wu. A survey on negative transfer. *IEEE Transactions on Neural Networks and Learning Systems*, 2021. doi: 10.1109/TNNLS.2021.3099090.
Yingqin Zhu, Yue Liu, Nan Wang, ZhaoZhao Zhang, and YuanQiang Li. Real-time error compension.

sation transfer learning with echo state networks for enhanced wind power prediction. *Applied Energy*, 379:124893, 2025, doi: 10.1016/j.apenergy.2024.124893.

Energy, 379:124893, 2025. doi: 10.1016/j.apenergy.2024.124893.